A Remarkably Loud Quasi-Periodicity after a Star is Disrupted by a Massive Black Hole

Dheeraj R. Pasham[1*], Ronald Remillard[1], Chris Fragile[2], Alessia Franchini[3], Nicholas Stone[4], Lodato Guiseppe[3], Eric Coughlin[4], Deepto Chakrabarty[1], Jeroen Homan[1], Fred Baganoff[1], Jack Steiner[1]

[1]MIT Kavli Institute, Cambridge, MA 02139
[2]Department of Physics and astronomy, College of Charleston, SC
[3]Department of Physics, University of Milan, Dipartimento di Fisica, Via Celoria 16
[4]Department of Physics, Columbia University, New York

[*]To whom correspondence should be addressed; E-mail: dheeraj@space.mit.edu

Immense tidal forces of massive black holes (MBHs) can rip apart stars that come too close to them. As the resulting stellar debris spirals inwards it heats up and emits x-rays when closest to the BH. Here, we report the discovery of an exceptionally stable 131-second x-ray quasi-periodicity from a MBH after it disrupts a star. Using a BH mass indicated from host galaxy scaling relations implies that, (1) this periodicity is the fastest/closest ever seen from a BH, and (2) the BH is rapidly spinning. Although the source x-ray properties are very similar to previously-known disruption events its observations were significantly more sensitive. Thus, high-sensitive observations of future events should enable periodicity detections which would in-turn constrain masses and spins of quiescent MBHs hidden at galaxy centers.

Almost all massive galaxies are expected to harbor a massive BH at their centers (*1*), yet

most of them are inactive and do not produce any observable radiative output. However, it is predicted that roughly once every few$\times 10^{4-5}$ years (*2–4*) a star would pass near to the BH and will get disrupted by the BH's gravitational forces. Such episodes, known as tidal disruption events (TDEs) (*5*), trigger accretion onto quiescent BHs and provide a brief window of opportunity to measure the two fundamental properties that define BHs: mass and spin. While there are empirical scaling laws to infer BH masses, for example, using host galaxy properties (*6*), the spins of massive BHs have been very difficult to constrain. This is because the effects of spin predicted by Einstein's theory of general relativity only emerge in the immediate vicinity of BHs, typically within a few gravitational radii* (*7*). Thus, BH spin measurements require studying radiation from the strong gravity regime comprising the innermost regions of the accretion flow. Theoretical models for TDEs predict that shortly after the disruption a fraction of the stellar debris settles into a hot inner disk that emits primarily in the soft x-rays (*8, 9*). Thus, identifying such disk-dominated/soft-state x-ray bright TDEs could provide a new avenue to measure spins of numerous BHs lying dormant in external galaxies. However until now, x-ray data of known soft-state TDEs lacked the sensitivity to probe this strong-gravity regime in-detail. Here, we report on an unprecedented event ASASSN-14li which has been observed by all major x-ray telescopes and has the most sensitive soft x-ray observations of a TDE to-date.

The spectacular transient event ASASSN-14li was discovered by an optical all-sky survey on 22 November 2014 (*3*). Soon after its discovery it became apparent that it exhibited nearly all properties of previously-known TDEs: spatial position consistent with the host galaxy's center (within 70$\pm$90 parsecs (*3*)), a power-law luminosity decline with time with an index of 5/3 (*10*) as expected from a TDE (*11*), a blue optical spectrum with broad Hydrogen and Helium emission lines and a constant optical color unlike any ordinary supernova (*3*). In addition to the optical and UV emission ASASSN-14li also produced an x-ray (*10*) and a radio synchrotron

*Gravitational radius, R_g = GM/c^2, where G, M, and c are the gravitational constant, BH mass, and the speed of light, respectively.

flare (*12, 13*). Owing to these multi-wavelength properties ASASSN-14li has been dubbed as the "Rosetta stone" for TDEs (*14*).

In particular, two properties of ASASSN-14li make it an intriguing event. Firstly, its BH mass is constrained to be in between $10^{5.8-7.1}$ $M_{\odot}$ using the existing scaling relations between BH mass and host galaxy properties (*3, 13, 15*). Secondly, its x-ray energy spectrum is blackbody-like (thermal) (*10, 16, 17*). The inferred size of the thermal x-ray emitting region is on the order of only a few gravitational radii (*10*) and remains roughly constant with time (*10, 16*). This strongly suggests that x-rays from ASASSN-14li originate from an inner accretion flow close to the BH.

In stellar-mass BHs, a sudden onset of accretion often excites quasi-periodic oscillations (QPOs) in the x-ray flux (*18*). In instances where the majority of the x-ray emission is dominated by the accretion disk, the QPO frequencies have enabled BH spin measurements (*19, 20*). We searched for a stable QPO in the soft x-ray band (0.3-1.0 keV) of ASASSN-14li by combining all its publicly-available data. We extracted an average power density spectrum (PDS) using both *XMM-Newton* and *Chandra* data taken in six different epochs during the first 450 d after ASASSN-14li's discovery (see Fig. 1 for its long-term x-ray evolution). The combined x-ray PDS shows a strong feature at 7.65$\pm$0.4 mHz (131-seconds; coherence, Q = centroid-frequency/QPO's-width $\approx$10). The QPO is highly statistically significant at greater than the 5σ level for a search at all frequencies (trials) below 0.1 Hz (see Fig. 2, left panel).

Moreover the QPO is independently detected in the averaged *XMM-Newton* and *Chandra* data with a significance of $>$4.4σ and $>$3σ, respectively, for a search including all frequencies/trials below 0.1 Hz (see supplement information, SI, Fig. S1). Because of data pile-up we can only estimate a lower limit on the QPO's fractional root-mean-squared (RMS) amplitude to be $>$2.2% in the *XMM-Newton* data. However, the *Chandra* observation was made roughly 420 d after the discovery, by which time ASASSN-14li's flux had declined by roughly a factor of

$\approx$ 10, and the pile-up was minimal (see SI). The QPO's fractional RMS amplitude in *Chandra* data was 59$\pm$11%. After establishing the QPO at 7.65 mHz, we also constructed an average *Swift* x-ray (0.3-1.0 keV) PDS. The strongest feature in the average *Swift* PDS is at 7.0$\pm$0.5 mHz and is consistent with the QPO detected in the *XMM-Newton* and *Chandra* datasets (Fig. 2, right panel).

A *Chandra* image shows only a single x-ray point source spatially coincident with the galaxy PGC043234 (SI Fig. S2). This allows us to assert that the QPO does not originate from a nearby contaminating source. Furthermore, the QPO is absent in the average background PDS (SI Fig. S1, bottom panels) and is detected by three different x-ray detectors. This establishes that the QPO is not an instrumental artifact and is indeed associated with ASASSN-14li. In addition, the supplement movie shows that the QPO signal improves gradually as more PDS are averaged. This implies that the QPO does not originate from a single epoch observation but is present throughout at least the first 450 d of the event. The average *Swift* PDS using data acquired over 500 d and the *Chandra* PDS from roughly day 420 also confirm that the QPO is present all throughout the first 450 d of the outburst. This implies that this high-amplitude QPO is remarkably stable for 3×10^5 cycles ($\approx$ 450 d/131 s). While the stability and coherence of the QPO is comparable to the soft-state QPOs of stellar-mass BHs, a modulation amplitude of $>$50% is unprecedented (*21*).

An alternative scenario in which the oscillation might be pulsations from a neutron star is rejected for the following reasons: large optical/UV and radio photospheric sizes (*3, 16, 17, 22*), high persistent bolometric luminosity (*16, 17*), very soft x-ray spectrum (*10, 16*), finite width of the QPO (see Fig. 1), and in general the multiwavelength properties of ASASSN-14li are strikingly similar to many previously-known TDEs and unlike any known neutron star outburst (see SI for more details).

It is known empirically that the masses of the central BHs are correlated with the properties

of their host galaxies (*6, 23*). For instance, the velocity dispersion of stars in the inner bulges of galaxies (σ) is correlated with the BH mass (M), and is commonly referred to as the M-σ relation. In addition, the total stellar mass in the bulge and the optical luminosity of the host galaxy are shown to correlate with the BH mass (*23, 24*). These empirical relations suggest that the BH in ASASSN-14li has a mass anywhere in between $10^{5.8-7.1}$ $M_{\odot}$ (*3, 13, 15*). This value is also consistent with mass derived from detailed physical modeling of ASASSN-14li's multi-waveband (x-ray, optical and UV) light curves (*10*). Assuming this BH mass, we compared the 7.65 mHz QPO frequency to the five possible frequencies of motion of a test particle orbiting a spinning BH in Kerr spacetime (*7, 20*).

All these five particle frequencies are determined by the BH's mass, spin and the radial distance of the emitting region. In soft-state stellar-mass BHs the inner edges of accretion disks extend to a constant radius for a wide range in accretion rates (*25*). The natural inner radius predicted from Einstein's theory of general relativity is the so-called innermost stable circular orbit (ISCO). Because ASASSN-14li also appears to be disk-dominated we started our frequency comparison using ISCO as the radial distance (Fig. 3). Surprisingly, even with the closest/fastest possible location, i.e, ISCO, the only solutions are the ones that require the BH to be rapidly spinning. A lower limit on BH's dimensionless spin parameter[†] can be calculated from the BH spin vs mass contours (Fig. 3). This corresponds to the intersection of the BH mass lower limit and the fastest frequency which at any given radius is the Keplerian frequency (blue in Fig. 3). This implies that ASASSN-14li's spin is greater than 0.7 (Fig. 3). Choosing any larger radius will only push this limit to a higher spin value.

Many researchers expect that a proper theory for disk oscillations must consider normal mode analyses for a detailed accretion flow in strong gravity. However, there is also an expectation that such oscillations would be slower than the dynamical frequency given by the azimuthal

[†] Jc/GM^2, where J is BH's angular momentum.

(Keplerian) frequency of a test particle located at the ISCO (*26*). The results in Fig. 3 therefore describe a lower limit to the spin of the MBH that caused the TDE. Furthermore, the mass vs spin contours in Fig. 3 allow us to derive an absolute upper limit on the black hole mass of $2\times10^6\ M_\odot$ corresponding to the maximum spin of a^*=0.998.

On the other hand, it is plausible that ASASSN-14li's host galaxy and the disrupting BH may not obey the empirical scaling laws and instead the BH mass could be significantly below a value of a few$\times10^5\ M_\odot$ (*27*). If that were the case, then the BH could also have a moderate spin. But, more interestingly, it would imply that the disrupting BH is a member of the rare class of intermediate-mass black holes which have been very challenging to find so far. In any case, to our knowledge, such a high-amplitude quasi-periodic phenomenon that is stable for years has never been seen before from any BH. The extreme phenomenon of TDEs is relatively new which we are only beginning to understand as more sensitive observations are becoming available. This discovery presents a new probe into the complex accretion physics of a star getting disrupted by a MBH and may require a new physical mechanism to explain its origin (see SI for some discussion).

Previously, Reis et al. (2012) (*28*) reported the first case of a periodicity (at $\approx$200-seconds) from a TDE SwJ1644+57. However, SwJ1644+57 is an atypical TDE where the entire electromagnetic radiation was dominated by a jet directly pointing along our line of sight (*29, 30*). Obviously, only a very small fraction of all TDEs would fortuitously align with our line of sight. Moreover, compared to ASASSN-14li, SwJ1644+57's periodicity was roughly 15 times weaker in amplitude and was present only for a short duration of at most a few weeks after its discovery. Therefore, it has been unclear if all TDEs should exhibit such quasi-periodic variations. Our discovery of a very loud (fractional RMS$>$50%), and more importantly very persistent (stable over years) quasi-periodicity from a poster-child TDE suggests that all TDEs could, in principle, exhibit such phenomenon. Because x-ray variations originate from the strongest

gravity regime in the immediate vicinity of BHs, their period stability then strongly argues that they encode information about the BH's fundamental properties (mass and spin). Thus, similar quasi-periodicity detections in future TDEs will not only probe general relativity in strong regime but may also allow us to build a census of BH demographics across the Universe.

Acknowledgments. Pasham would like to thank David Huenemoerder and Adam Ingram for valuable discussions. This work is based on observations made with *XMM-Newton*, *Chandra*, and *Swift*. *Swift* is a mission that is managed and controlled by NASA's Goddard Space Flight Center (GSFC) in Greenbelt, Maryland, USA. The data used in the present article is publicly available through NASA's *HEASARC* archive.

All the data presented here is public and can be found in the ESA/*XMM-Newton*, NASA/*Chandra* and *Swift* archives:
http://nxsa.esac.esa.int/nxsa-web/
http://cxc.harvard.edu/cda/
http://heasarc.nasa.gov/docs/swift/archive/

Supplement Material
Figs. S1 to S2
References (31-38)

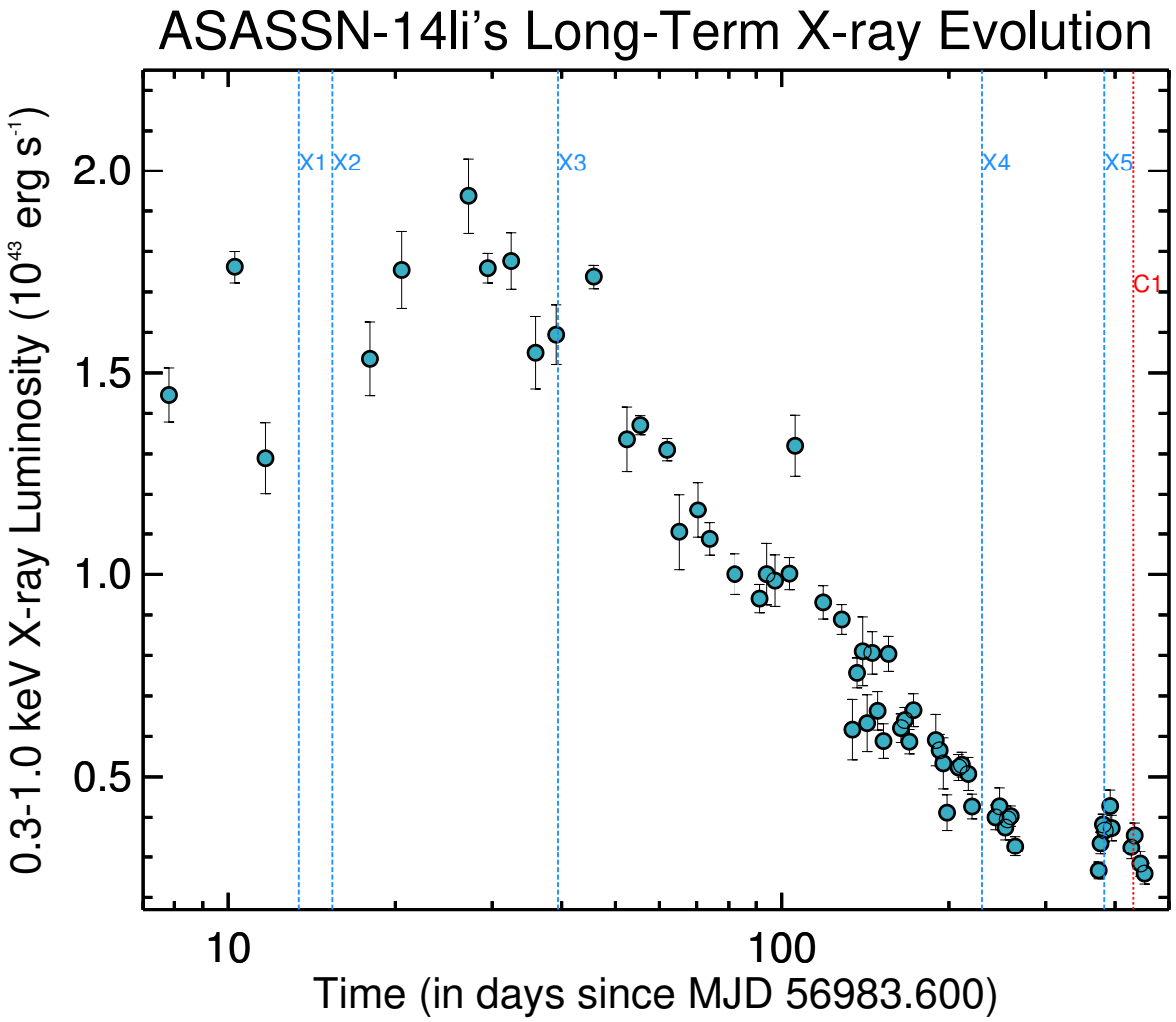

Figure 1: **ASASSN-14li's long-term x-ray light curve.** The data were taken with *Swift*/XRT (see SI). The dashed vertical blue lines marked as Xn (n=1 to 5) represent the five epochs of *XMM-Newton* observations. The dotted vertical red line (C1) shows the epoch of *Chandra*/ACIS observation.

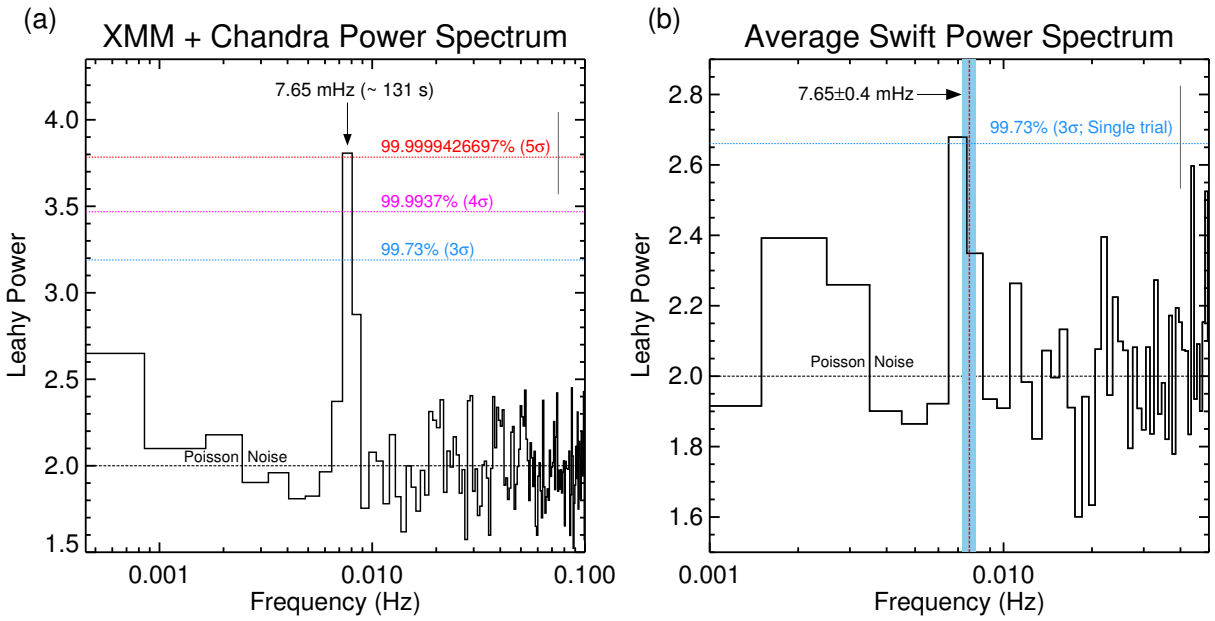

Figure 2: **ASASSN-14li's x-ray QPO at 7.65 mHz is detected by three different telescopes:** *XMM-Newton*, *Chandra* **and** *Swift*. **(a)** ASASSN-14li's averaged x-ray PDS using eight continuous 10,000 s light curves taken with *XMM-Newton* and *Chandra*/ACIS. The frequency resolution is 0.8 mHz. The strongest feature in the power spectrum lies at a frequency of 7.65±0.4 mHz (≈131-seconds). The dashed horizontal blue, magenta, and red lines represent the 3, 4, and 5σ statistical contours. A characteristic 1σ error bar is shown as a grey bar. Independently, the QPO is evident at the 4.4σ and the 3σ levels in the averaged *XMM-Newton* and *Chandra*/ACIS, respectively (see SI Fig. S1). **(b)** Average Swift/XRT PDS. *Swift*/XRT's effective area is roughly $1/20^{th}$ that of *XMM-Newton*. Nevertheless, we evaluated the average XRT PDS using the entire archival data. We used 85 continuous 1000 s light curves with a frequency resolution is 1 mHz. The horizontal line shows the 3σ contour assuming–a single trial–search at 7.65 mHz. The highest peak in the power spectrum is at 7.0±0.5mHz and is consistent with the most prominent feature in the *XMM-Newton* and the *Chandra* power spectra (SI Fig. 1).

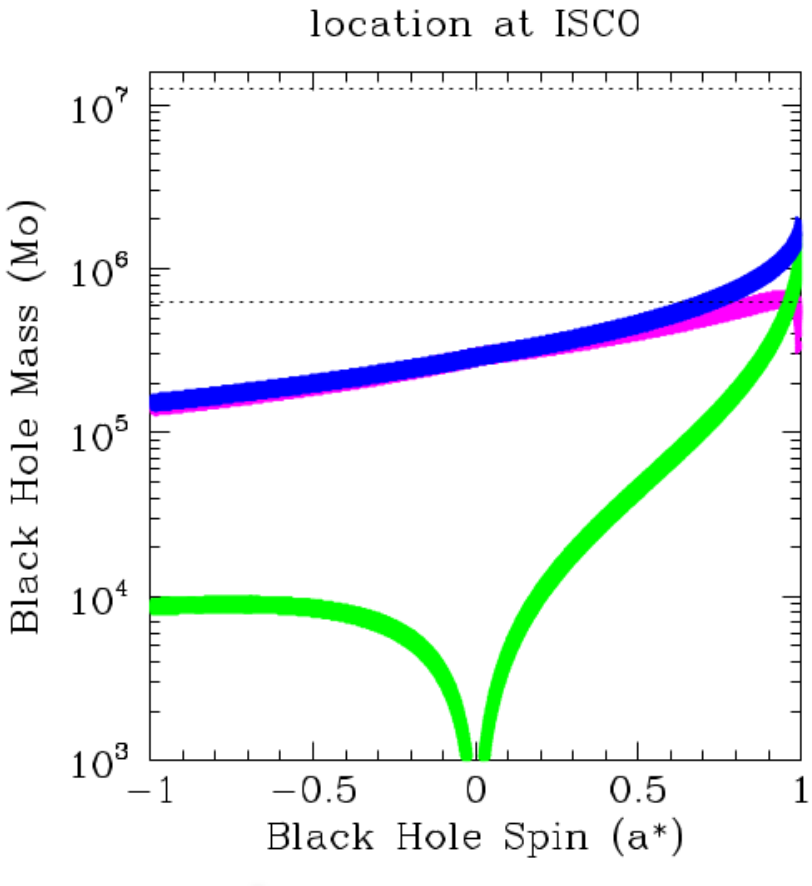

Figure 3: **Black Hole dimensionless spin parameter vs mass contours:** Spin vs mass contours assuming the 7.65 mHz QPO is associated with any of the three particle frequencies: Keplerian frequency (ν_ϕ, blue), azimuthal epicyclic frequency (ν_θ, magneta) and Lense-Thirring precession (ν_ϕ - ν_θ, green) at the innermost stable circular orbit (ISCO). At ISCO the radial epicyclic frequency (ν_r) is zero and the periastron precession frequency (ν_ϕ - ν_r) is thus equal to the Keplerian frequency (see SI). The widths of these contours reflect the error in the QPO's centroid of 0.8 mHz. The dotted horizontal lines show ASASSN-14li's BH mass ($10^{5.8-7.1}$ $M_\odot$) estimated from its host galaxy scaling relations. The only formal solutions are the ones that require the BH spin to be greater than 0.7.

References

1. D. Richstone, *et al.*, *Nature* **395**, A14 (1998).
2. N. C. Stone, B. D. Metzger, *Mon. Not. R. Astron. Soc.* **455**, 859 (2016).
3. T. W.-S. Holoien, *et al.*, *Mon. Not. R. Astron. Soc.* **455**, 2918 (2016).
4. S. van Velzen, G. R. Farrar, *Astrophys. J.* **792**, 53 (2014).
5. M. J. Rees, *Nature* **333**, 523 (1988).
6. K. Gültekin, *et al.*, *Astrophys. J.* **698**, 198 (2009).
7. J. M. Bardeen, W. H. Press, S. A. Teukolsky, *Astrophys. J.* **178**, 347 (1972).
8. G. Lodato, E. M. Rossi, *Mon. Not. R. Astron. Soc.* **410**, 359 (2011).
9. C. S. Kochanek, *Astrophys. J.* **422**, 508 (1994).
10. J. M. Miller, *et al.*, *Nature* **526**, 542 (2015).
11. E. S. Phinney, *The Center of the Galaxy*, M. Morris, ed. (1989), vol. 136 of *IAU Symposium*, p. 543.
12. K. D. Alexander, E. Berger, J. Guillochon, B. A. Zauderer, P. K. G. Williams, *Astrophys. J.* **819**, L25 (2016).
13. S. van Velzen, *et al.*, *Science* **351**, 62 (2016).
14. J. Krolik, T. Piran, G. Svirski, R. M. Cheng, *Astrophys. J.* **827**, 127 (2016).
15. T. Wevers, *et al.*, *Mon. Not. R. Astron. Soc.* **471**, 1694 (2017).
16. J. S. Brown, *et al.*, *Mon. Not. R. Astron. Soc.* **466**, 4904 (2017).
17. D. R. Pasham, *et al.*, *Astrophys. J.* **837**, L30 (2017).
18. J. E. McClintock, R. A. Remillard, *Black hole binaries* (2006), pp. 157–213.
19. A. Franchini, S. E. Motta, G. Lodato, *Mon. Not. R. Astron. Soc.* **467**, 145 (2017).
20. S. E. Motta, T. M. Belloni, L. Stella, T. Muñoz-Darias, R. Fender, *Mon. Not. R. Astron. Soc.* **437**, 2554 (2014).
21. J. Homan, *et al.*, *Astrophys. J. Suppl.* **132**, 377 (2001).
22. D. R. Pasham, S. van Velzen, *ArXiv e-prints* (2017).
23. N. J. McConnell, C.-P. Ma, *Astrophys. J.* **764**, 184 (2013).

24. L. Ferrarese, H. Ford, *Space Sci. Rev.* **116**, 523 (2005).

25. J. F. Steiner, *et al.*, *Astrophys. J.* **718**, L117 (2010).

26. T. E. Strohmayer, *Astrophys. J.* **554**, L169 (2001).

27. J. E. Greene, *et al.*, *Astrophys. J.* **721**, 26 (2010).

28. R. C. Reis, *et al.*, *Science* **337**, 949 (2012).

29. J. S. Bloom, *et al.*, *Science* **333**, 203 (2011).

30. A. Tchekhovskoy, B. D. Metzger, D. Giannios, L. Z. Kelley, *Mon. Not. R. Astron. Soc.* **437**, 2744 (2014).

Supplementary Information

1 Data Reduction.

The data used in this work has been acquired by three different x-ray telescopes: *Swift*, *XMM-Newton*, and *Chandra*. The X-Ray Telescope (XRT) on board *Swift* started monitoring ASASSN-14li roughly a week after its discovery by the All-Sky Automated Survey for Supernovae (ASAS-SN (*31*)) on MJD 56983.6 (*3*). Since discovery on 22 November 2014 until May 2017, *Swift* observed ASASSN-14li on over 100 occasions with each observation lasting between a few 100 to 1000 seconds long. *XMM-Newton* and *Chandra*–with effective areas larger than the XRT–provided fewer but more sensitive observations each lasting anywhere between 10,000 and 90,000 seconds.

We started our analysis with *Swift*/XRT data to assess the long-term x-ray evolution as follows. As noted by earlier works (*10, 17*), the individual XRT data sets are indeed piled-up. To mitigate the effect of pile-up we extracted event lists from an annulus region centered on the source by excluding an inner pile-up radius in each individual observation by following the procedure outlined by the XRT pile-up guide[‡]. The individual XRT observations only have a few counts and thus cannot be used to constrain the spectral shape. Therefore, we extracted average energy spectra by combining neighboring observations until a total of 3000 counts were reached. Similar to earlier works (*10*) we modeled each energy spectrum with an absorbed black body modified by red-shift of the host galaxy and implemented it in the x-ray SPECtral fitting package, XSPEC (*32*), as `phabs*(zashift(phabs*bbodyrad)`. Consistent with earlier works (*10, 16*), we found that the shape of ASASSN-14li's x-ray energy spectrum remained more or less constant. We estimated the flux and thus the luminosity in each individual *Swift* observation by fitting it with the same black body function but fixed the column density and disk temperature value to the nearest (in time) averaged spectral values (see Pasham & van Velzen 2017, submitted, for more specific details and the best-fit model parameters). ASASSN-14li's final XRT long-term light curve is shown in Fig. 1.

XMM-Newton and *Chandra* observed ASASSN-14li on multiple occasions with six and three data sets publicly available at the time of writing of this paper. However, one of the *XMM-Newton* observations (obsID: 0770980501) was severely effected by background flaring and two of the *Chandra* data sets carried out with the High-Resolution Camera (HRC) were background dominated. Therefore, we did not consider these data sets for further analysis. After this initial screening we were left with five *XMM-Newton* and one *Chandra* observation. The vertical lines in Fig. 1 mark the epochs of these observations.

We used the *XMM-Newton* Standard Analysis System (`xmmsas`: version 15.0.0) to extract the images and the event lists from all the five *XMM-Newton* data sets. Because the detection

[‡]http://www.swift.ac.uk/analysis/xrt/pileup.php

sensitivity of a quasi-periodic feature in the light curves increases sharply with the count rate (*33*), we combined the data acquired by all the three detectors (pn, MOS1 and MOS2) on board the European photon imaging camera (EPIC) and considered only those epochs during which all the three detectors were operating. We started our analysis by reducing/reprocessing the datasets to extract the level-2 event-lists. We first extracted images of ASASSN-14li's field of view and visually confirmed that there are no contaminating sources nearby. We extracted source events from a circular region of radius 40" centered on the source. All the observations were taken in a small window mode to enable faster readout. To better constrain the background variability, events were extracted from two circular regions of radius 70" and away from the source. A significant fraction of these data sets were affected by background flaring. Because these high-amplitude background flux variations can sometimes manifest as quasi-periodic features in the power spectra we carefully removed these high background flux epochs from our analysis. This resulted in a number of good time intervals in each individual observations.

As noted by earlier studies (*10*), the source is also piled-up in the *XMM-Newton* observations. However, for the purposes of extracting power density spectra this translates to a reduction in the count rate and thus a reduction in the fractional root mean-squared (RMS) amplitude of any quasi-periodic oscillation (QPO). Furthermore, pile-up effects are more severe for x-ray hard sources. ASASSN-14li, on the other hand, has a very soft x-ray spectrum with almost all photons below 1 keV (*10*). To alleviate the pile-up issue and at the same time not compromise on the count rate, we considered all single pixel events (`PATTERN==0`) within a 40" circular region with energies in the range of 0.3-1.0 keV for power spectral analysis.

We then extracted an image and an event list from *Chandra*'s Advanced CCD Imaging Spectrometer (ACIS) using the Chandra Interactive Analysis of Observations tool called `ciao`. Currently, *Chandra* offers the best spatial resolution in x-rays. We inspected ASASSN-14li's ACIS image–with a spatial resolution of 0.5"–and found that it is the only source in that field of view. This is shown in Fig. S1. Source events were extracted from a circular region of radius 2.5" centered on the source while the background events were extracted from a region significantly ($\gtrsim$ 3000 times) larger than the source region. Again we utilized only single pixel events in the calibrated energy range of 0.4-1.0 keV.

2 Power Spectral Analysis.

We first divided the data into 10,000-second continuous segments and extracted their light curves with a 1-second resolution. We then constructed a Leahy normalized (*34*) power density spectrum (PDS)–where the mean Poisson noise level is 2–from each of the 10,000 second light curves. This resulted in eight PDS which were all combined to obtain an average PDS of ASASSN-14li over its 500 d flare duration (see Fig. 1).

The most prominent feature in the PDS is a QPO at roughly 7.65 mHz while the rest of the power spectrum is consistent with Poisson noise (see left panel of Fig. 2). We estimated its statistical significance as follows. First, we ensured that the mean noise level was equal to 2 as this

is the value expected from pure Poisson (white noise) process. We then computed the probability, at the 99.73% (3σ), the 99.9937% (4σ), and the 99.9999426697% (or 5σ) confidence levels, of obtaining the power, P = $P_* \times 8 \times 8$ from a χ^2 distribution with $2 \times 8 \times 8$ degrees of freedom. Here P_* is the power value of a statistical fluctuation at a given confidence level. This χ^2 distribution was used because we averaged in frequency by a factor of 8 and averaged 8 individual power spectra. Considering all the trials below 0.1 Hz we computed the 3σ (1/(371$\times$trials)), the 4σ (1/(15787$\times$trials)) and the 5σ (1/(1744278$\times$trials)) confidence contours. These are shown as the blue, magenta and the red contours, respectively, in the left panel of Fig. 2. The highest bin in the feature at 7.65 mHz is greater than the 5σ confidence level and is thus highly statistically significant.

We also extracted a PDS of the background in the exact same procedure as above and found it to be consistent with a white noise process.

2.1 Separate *XMM-Newton* and *Chandra* PDS.

After establishing the QPO at 7.65 mHz we extracted an average PDS separately from *XMM-Newton* and *Chandra* data. These are shown in the top-left and the top-right panels of the SI Fig. S1. The 7.65 mHz QPO is evident in both the detectors and is significant at the 4.4σ and the 3σ level assuming a search considering all trials below 0.1 Hz.

The fact that the QPO is present in two different detectors at different epochs is already ensuring that it is detector-independent and is not a manifestation of the background variability. Nevertheless, we extracted the average *XMM-Newton* and *Chandra* PDS of the background sky in exactly the same manner as the source, i.e., same light curve length and frequency binning. These are shown in the bottom two panels of Fig. 1. It is evident that there is no indication of a QPO in the background light curves.

2.2 Stacked *Swift*/XRT PDS.

The XRT on board *Swift* has an effective area[§] of $\lesssim 1/20^{th}$ that of *XMM-Newton*/EPIC's combined pn+MOS[¶]. Nevertheless, using 1000-second light curve segments spread across the $\gtrsim$ 450 d flare we constructed an average 0.3-1.0 keV PDS. The QPO at 7.65 mHz is recovered at over the 3σ (single trial) confidence level. This is shown in the right panel of Fig. 2. This again suggests that the QPO was stable over the first 450 d since its discovery.

2.3 The 7.65 mHz QPO is stable.

The fact that the 7.65 mHz QPO is present in the average PDS of eight observations scattered over 450 d already demonstrates that the QPO is stable throughout the 450 d flare. To establish this further we constructed a dynamic PDS where we show the progress of the PDS as we add

[§]https://swift.gsfc.nasa.gov/about_swift/xrt_desc.html

[¶]https://xmm-tools.cosmos.esa.int/external/xmm_user_support/documentation/uhb/epicfilters.html

one additional PDS (see supplement movie). This demonstrates clearly that the 7.65 mHz QPO does not originate from a single observation that dominates the average PDS. Instead the signal gradually improves as more and more data is added. This suggests that the signal is present in all the individual *XMM-Newton* and *Chandra* power spectra. Furthermore, the average *Swift* PDS taken over 450 d also suggests the QPO has to be stable.

3 QPO's Coherence and fractional RMS amplitude

The coherence of the QPO (centroid frequency (ν)/width ($\Delta\nu$)) as measured from the combined *XMM-Newton* and *Chandra* power spectrum (Fig. 2) is greater than 0.00765/0.0008 $\approx$ 10.

Because all the *XMM-Newton* observations are piled-up we can only get a lower-limit on the QPO's fractional RMS from these datasets. The lower-limit on the QPO's RMS from the combined *XMM-Newton* observations is 2.2%. On the other hand, the *Chandra*/ACIS data is not effected by pile-up and thus gives an accurate estimate of the fractional RMS to be 59$\pm$11%.

4 Estimating *Chandra*/ACIS Pile-up Fraction

The mean count rate during the *Chandra* observation (C1 in Fig. 1) was only roughly 0.008 counts/sec. At such low count rates pile-up is expected to be minimal. Nevertheless, we estimated the pile-up fraction using the `ciao` tool `pileup_map`. Using the counts/frame in the brightest pixel in the pile-up image generated from this tool we calculated the pile-up fraction to be only $\approx$ 4.5% (see Eq. 3 of pile-up analysis guide[‖]). Using PIMMS[**] also gives a similar value. In summary, because the *Chandra* data were not severely piled-up we could estimate the RMS value of the QPO during the C1 epoch in Fig. 1.

5 Ruling out a Pulsar Origin

A pulsar origin for ASASSN-14li–and thus the QPO–is unlikely for the following many reasons.

1. Firstly, the size of ASASSN-14li's optical/UV photosphere ($\sim 10^{14}$ cms (*16, 17*)) is a factor of $\gtrsim 10^5$ larger than the characteristic emission size of a $2M_\odot$ neutron star's accretion disk of a few thousand gravitational radii. A stellar-mass BH origin can also be ruled out on the same basis.

2. Secondly, ASASSN-14li's radio emission is not dominated by emission from a neutron star. Its radio spectral energy distributions are consistent with synchrotron self-absorption with a characteristic emission size of a few$\times 10^{16}$ cms (*12, 22*). Again, this is several orders of magnitude large than a typical neutron star's size of roughly 10^6 cms.

[‖] http://cxc.harvard.edu/csc/memos/files/Davis_pileup.pdf

[**] http://cxc.harvard.edu/toolkit/pimms.jsp

3. ASASSN-14li's host galaxy distance of 90.3 Mpcs (*3*) would imply that the putative neutron star is emitting at an apparent bolometric (x-ray+optical+UV) luminosity $>3\times10^6$ its Eddington limit. This is plausible in light of the recent discovery of so-called ultra-luminous x-ray (ULX) pulsars (*35*) with maximum luminosities upto 7×10^{40} erg/sec. However, ASASSN-14li would still be an extreme ULX pulsar with a factor of >1400 brighter than even the most luminous ULX pulsar (*36*). Moreover, all three known ULX pulsars and the bursting pulsar GRO J1744-28 (*37*) are highly variable (*35, 36*). They reach super-Eddington luminosities only for brief periods of a few days at a time (*35, 36*). ASASSN-14li on the other hand has an average apparent bolometric luminosity of $>5\times10^{43}$ erg/sec or $\approx2\times10^5$ times Eddington for a neutron star for over at least two years after its discovery (*16*).

4. Also, ASASSN-14li's x-ray spectrum is unlike any ULX pulsar. Because all X-ray bright jets show hard x-rays, if ASASSN-14li's x-ray emission were highly beamed one would expect hard x-rays to be present. This is contrary to the observed very soft x-ray spectrum (*10, 17*).

5. The observed 7.65 mHz feature has a finite width (Fig. 2; coherence$\approx$10)) unlike a pulsar's signal that is expected to be highly coherent.

6. In principle, ASASSN-14li could be a foreground pulsar that happened to spatially coincide with a background galaxy. This would be highly coincidental especially because there are no known pulsars in this sky region (*38*). Nevertheless, we estimated the chance coincidence with a background galaxy as:

$$\frac{N_{gals} \times \pi R_{x\text{-}ray}^2}{\pi R_{gal}^2} \tag{S1}$$

   where N_{gals} is the number of galaxies within an circle of radius R_{gal} and centered on ASASSN-14li. $R_{x\text{-}ray}$ is the typical positional uncertainty of *Chandra*/ACIS which has been estimated to be 0.8" (90% positional accuracy[††]). Using the galaxy catalog from the Sloan Digital Sky Survey (data release 14) we find N_{gals}=1505 within a circular area of radius 10'. This translates to a chance coincidence of less than 3%. The mean and the lowest g-band magnitude of galaxies around ASASSN-14li is 22.9 and 28.4, respectively while ASASSN-14li's host galaxy–prior to the TDE–had a g-band magnitude of 16.1 (*3*). We repeated this estimate with a sky area of π5'$\times$5' and π15'$\times$15' to find that the resulting chance probabilities are the same. We stress that the above 3% estimate can be considered conservative (upper limit) as it includes chance coincidence with any part of the galaxy not just the center.

7. Finally, ASASSN-14li's multiwavelength properties are unlike any neutron star outburst

[††]http://cxc.harvard.edu/cal/ASPECT/celmon/

and are all similar to many previously known TDEs. A pulsar origin would only then compel us to conclude that all previously-known TDEs are foreground x-ray pulsars that perfectly coincided with background galaxies, which seems even more unlikely.

6 Description of the Five Frequencies of Motion around a Black Hole

A test particle moving in the strong gravity of a black hole has three fundamental frequencies. The fastest at any given radius is the Keplerain orbital frequency (ν_ϕ) for motion in the equatorial plane. Off-equatorial perturbations can induce two additional frequencies in the radial and the azimuthal directions. These are known as the radial (ν_r) and the azimuthal epicyclic (ν_θ) frequencies, respectively. Furthermore, beating between these three coordinate frequencies can lead to two additional frequencies: ν_{LT} = ν_ϕ - ν_θ and ν_{per} = ν_ϕ - ν_r. These are known as the Lense-Thirring precession and the periastron precession frequencies, respectively. The frequencies are defined as follows:

$$\nu_\phi = \pm \frac{\mathrm{c}^3}{2\pi \mathrm{GM}} \left[\frac{1}{\mathrm{r}^{3/2} \pm \mathrm{a}} \right] \tag{S2}$$

where r is the radius in units of gravitational radius, R_g = GM/c^2. G, M, and c are the gravitational constant, black hole mass, and the speed of light, respectively. a is the black hole's dimensionless spin parameter defined as a = J/(GM/c^2). J is the black hole's angular momentum.

$$\nu_\theta = \nu_\phi \left[1 \mp \frac{4a}{r^{3/2}} + \frac{3a^2}{r^2} \right] \tag{S3}$$

$$\nu_\mathrm{r} = \nu_\phi \left[1 - \frac{6}{r} \pm \frac{8a}{r^{3/2}} - \frac{3a^2}{r^2} \right] \tag{S4}$$

The upper and lower signs in the above equations refer to the prograde and retrograde orbits, respectively (See Motta et al. (2014) (*20*) and Franchini et al. 2016 (*19*) for more details).

7 Discussion of a Plausible QPO Mechanism

In general, because the star can approach the disrupting BH from any direction, its orbital plane/angular momentum is expected to be arbitrarily oriented with respect to the BH's spin axis. Hence the accretion disk that forms after the disruption is also expected to be initially misaligned with respect to the BH's spin. Therefore, it has been predicted (*39*) that the asymmetric spacetime around a spinning BH should force such a misaligned disk to precess and produce quasi-periodic modulation in the soft x-ray flux. Assuming the observed 7.65 mHz

QPO originates from the precession of a newly-formed accretion disk would then imply that the precessing disk/ring is very narrow. Using the semi-analytical approach for a precessing TDE disk as formulated by (*40*), for a BH mass between 10^4 and 10^7 $M_\odot$, the implied radial extent of the disk is between a few tens to a fraction of an R_g, respectively, for maximally spinning BHs. Even narrows disks are required for smaller spin values. In fact some theoretical works including (*41, 42*) have predicted the occurrence of such long-lived discrete, narrow precessing rings around misaligned accretion flows. However, such systems are yet to be realized in full 3-dimensional general relativistic magneto-hydrodynamic (GRMHD) simulations. Also, in order to produce such narrow disks it would require the stellar debris to plunge deep into the gravitational potential of the BH. The so-called penetration parameter, β, (*43*), defined as the ratio of the tidal radius (the radius at which the BH's tidal forces exceed the star's internal pressure) and the pericenter radius (radius of star's closest approach) measures how close the star plunges to the BH. For ASASSN-14li, if disk precession is the origin of the QPO, the penetration parameter would have to be high. For a 10^6 $M_\odot$ BH β has to be greater than 150, which corresponds to a maximally spinning BH. β increases to a few hundreds for lower spins. For a BH mass as low as 10^4 $M_\odot$ a maximally spinning BH would require a β-parameter of roughly 25 while a moderately spin of 0.5 would require a β value of roughly 80. As the probability of a TDE with an penetration parameter value of β_* is $1/\beta_*$ (ref), the above high values then imply that the stellar disruption in ASASSN-14li is low-probability event and thus would have to be highly fortuitous.

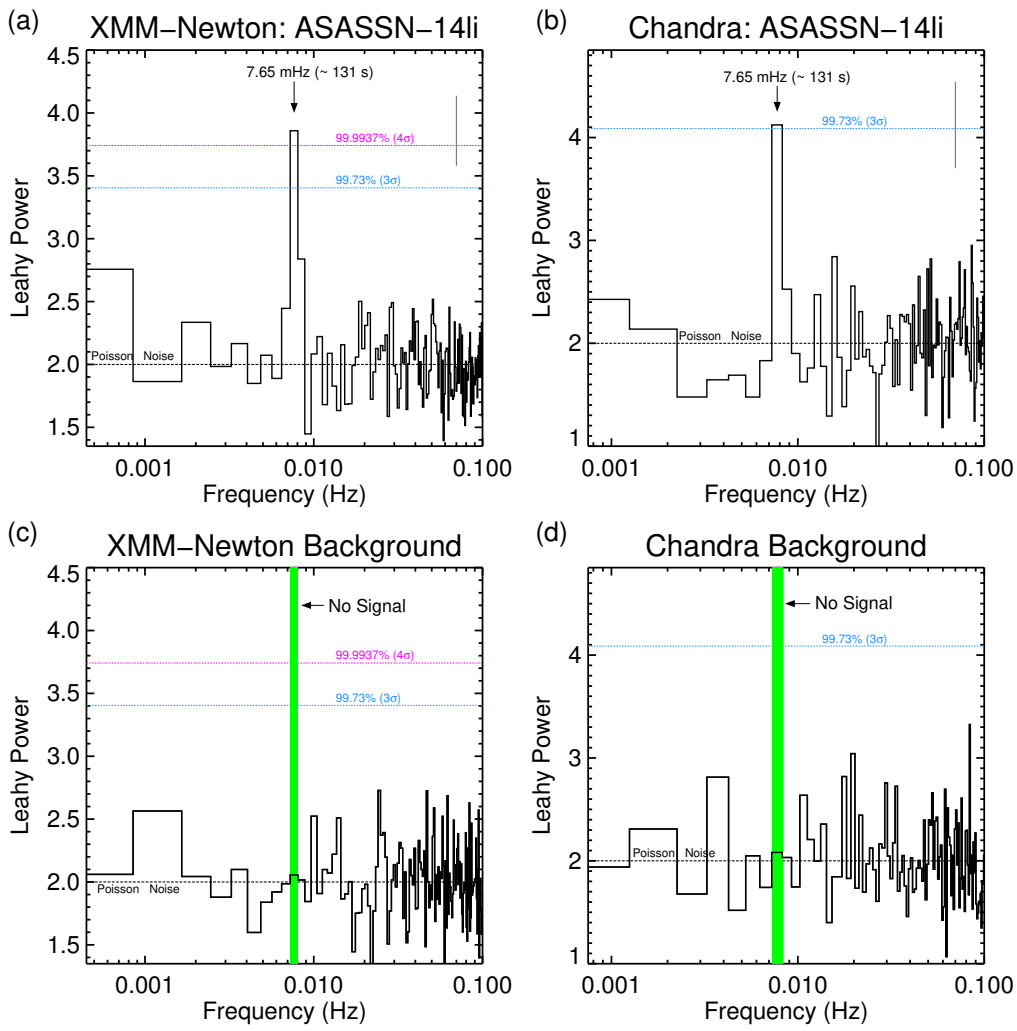

Figure S1: *XMM-Newton* **and** *Chandra* **power spectra of ASASSN-14li and backgrounds. (a)** ASASSN-14li's average x-ray (0.3-1.0 keV) power density spectrum using six continuous 10,000 s light curves taken with *XMM-Newton*. The frequency resolution is 0.8 mHz. The strongest feature in the power spectrum lies at a frequency of 7.65±0.4 mHz (≈ 131 seconds). The dashed horizontal lines represent the 3 and the 4σ statistical contours. A characteristic 1σ error bar is shown as a grey bar. **(b)** ASASSN-14li's x-ray (0.4-1.0 keV) power density spectrum using twelve 2,000 s light curves taken with *Chandra*'s ACIS instrument. The frequency resolution is 1 mHz. The strongest feature again lies at 7.75±0.5 mHz and is consistent with the most prominent feature in the average *XMM-Newton* spectrum (see **(a)**). **(c, d)** The PDS of the background light curves taken with *XMM-Newton* and *Chandra*/ACIS. The PDS were evaluated in the same manner as their respective source power spectra (top panels), i.e., same light curve length and frequency resolution. The vertical green band shows the location of the 7.65 mHz QPO and is clearly absent in both the *XMM-Newton* and the *Chandra* background light curves.

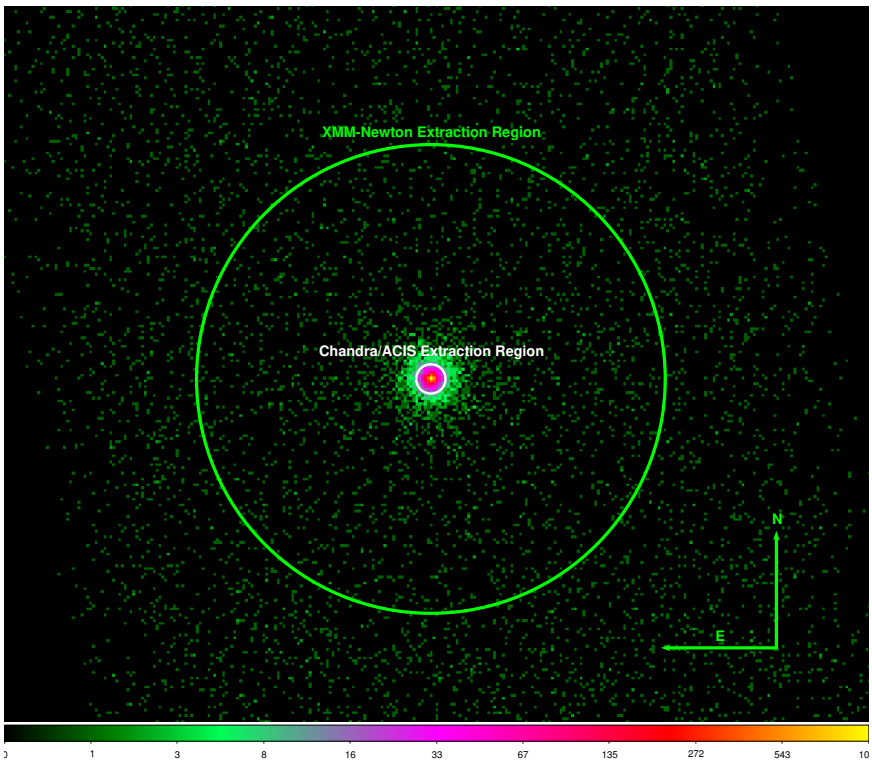

Figure S2: **Chandra/ACIS x-ray image of ASASSN-14li shows no contaminating sources.** It is clear that there is only one source, ASASSN-14li, and no obvious evidence for source contamination. *Chandra* and *XMM-Newton* extraction regions are shown as white (2.5") and green (40") circles, respectively.

References

31. B. J. Shappee, *et al.*, *Astrophys. J.* **788**, 48 (2014).

32. K. A. Arnaud, *Astronomical Data Analysis Software and Systems V*, G. H. Jacoby, J. Barnes, eds. (1996), vol. 101 of *Astronomical Society of the Pacific Conference Series*, p. 17.

33. M. van der Klis, *Timing Neutron Stars, eds. H. Ogelman and E.P.J. van den Heuvel. NATO ASI Series C, Vol. 262, p. 27-70. Dordrecht: Kluwer, 1988.* (1988), vol. 262, pp. 27–70.

34. D. A. Leahy, *et al.*, *Astrophys. J.* **266**, 160 (1983).

35. M. Bachetti, *et al.*, *Nature* **514**, 202 (2014).

36. G. L. Israel, *et al.*, *Science* **355**, 817 (2017).

37. K. Jahoda, *et al.*, *Nuclear Physics B Proceedings Supplements* **69**, 210 (1999).

38. R. N. Manchester, G. B. Hobbs, A. Teoh, M. Hobbs, *Astron. J.* **129**, 1993 (2005).

39. N. Stone, A. Loeb, *Physical Review Letters* **108**, 061302 (2012).

40. A. Franchini, G. Lodato, S. Facchini, *Mon. Not. R. Astron. Soc.* **455**, 1946 (2016).

41. C. Nixon, A. King, D. Price, J. Frank, *Astrophys. J.* **757**, L24 (2012).

42. G. Lodato, D. J. Price, *Mon. Not. R. Astron. Soc.* **405**, 1212 (2010).

43. N. Stone, R. Sari, A. Loeb, *Mon. Not. R. Astron. Soc.* **435**, 1809 (2013).